LRP2 in ependymal cells regulates BMP signaling in the adult neurogenic niche

Chandresh R. Gajera[1], Helena Emich[1], Oleg Lioubinski[1], Annabel Christ[1], Ruth Beckervordersandforth-Bonk[2], Kazuaki Yoshikawa[3], Sebastian Bachmann[4], Erik Ilsø Christensen[5], Magdalena Götz[2], Gerd Kempermann[6], Andrew S. Peterson[7], Thomas E. Willnow[1,*] and Annette Hammes[1]

[1]Max-Delbrück-Center for Molecular Medicine, Robert-Rössle-Str. 10, D-13125 Berlin, Germany
[2]Institute for Stem Cell Research, Helmholtz Center Munich, and Physiological Genomics, University of Munich, D-80336 Munich, Germany
[3]Institute for Protein Research, Osaka University, Osaka 565-0871, Japan
[4]Institute for Vegetative Anatomy, Charité Universitätsmedizin, D-10115 Berlin, Germany
[5]Institute of Anatomy, University of Aarhus, DK-8000C Aarhus, Denmark
[6]Center for Regenerative Therapies Dresden, Genomics of Regeneration, D-01307 Dresden, Germany
[7]Department of Molecular Biology, Genentech Inc., South San Francisco, CA 94080, USA
*Author for correspondence (willnow@mdc-berlin.de)

Accepted 23 March 2010
Journal of Cell Science 123, 1922-1930

doi:10.1242/jcs.065912

Summary

The microenvironment of growth factors in the subependymal zone (SEZ) of the adult brain provides the instructive milieu for neurogenesis to proceed in this germinal niche. In particular, tight regulation of bone morphogenetic protein (BMP) signaling is essential to balance proliferative and non-proliferative cell fate specification. However, the regulatory pathways that control BMP signaling in the SEZ are still poorly defined. We demonstrate that LRP2, a clearance receptor for BMP4 is specifically expressed in ependymal cells of the lateral ventricles in the adult brain. Intriguingly, expression is restricted to the ependyma that faces the stem cell niche. Expression is not seen in ependyma elsewhere in the lateral ventricles or in the dentate gyrus, the second major neurogenic zone of the adult brain. We further show that lack of LRP2 expression in adult mice results in impaired proliferation of neural precursor cells in the SEZ resulting in decreased numbers of neuroblasts reaching the olfactory bulb. Reduced neurogenesis coincides with increased BMP4 expression and enhanced activation of downstream mediators phospho-SMAD1/5/8 and ID3 in the stem cell niche. Our findings suggest a novel mechanism whereby LRP2-mediated catabolism of BMP4 in the ependyma modulates the microenvironment of the SEZ and enables adult neurogenesis to proceed.

Key words: Adult neurogenesis, LDL-receptor related receptors, Endocytosis, BMP4

Introduction

In the adult mammalian brain, neurons are continuously generated in two germinal niches: the subependymal zone (SEZ) of the lateral ventricles (Merkle and Alvarez-Buylla, 2006; Ninkovic and Gotz, 2007) and the subgranular zone (SGZ) of the hippocampus (Ehninger and Kempermann, 2008). In recent years the morphological events underlying adult neurogenesis have been described, but the signals that orchestrate the formation of newborn neurons are incompletely understood. However, it is appreciated that the milieu of growth factors and morphogens in the neurogenic stem cell niche is critical to this process (Lledo et al., 2008).

Although there are distinct differences in the processes that regulate embryonic and adult neurogenesis in mammals, there are also remarkable similarities. Thus, fine-tuning of competing signals provided by sonic hedgehog (SHH) and bone morphogenetic proteins (BMP) are central to the regulation of neural stem cell proliferation both in the embryonic neural tube and in the adult SEZ (Balordi and Fishell, 2007; Bertrand and Dahmane, 2006; Kriegstein and Alvarez-Buylla, 2009; Lim et al., 2000; Machold et al., 2003; Sur and Rubenstein, 2005).

The low-density lipoprotein receptor-related protein 2 (LRP2) is a receptor that plays an important role in balancing signals provided by SHH and BMP4 in the developing neural tube. In the early embryo, LRP2 is expressed on the apical surface of the neuroepithelium (Assemat et al., 2005; Spoelgen et al., 2005). Absence of *Lrp2* expression in mutant mice results in fusion of the forebrain hemispheres, a syndrome defined as holoprosencephaly (HPE) (Willnow et al., 1996). The underlying molecular defect has been linked to abnormal patterning of the neural tube caused by increased activity of BMP4 in the dorsal forebrain and loss of *Shh* expression in the rostroventral forebrain. These findings place LRP2 upstream of SHH and BMP signaling pathways in regulating early pattern formation and embryonic neurogenesis (Fuccillo et al., 2006; Spoelgen et al., 2005).

Interestingly, expression of LRP2 persists in the ventricular system of the adult brain (Zheng et al., 1994). Given its critical role in balancing key neurogenic pathways during development, we investigated its role in adult neurogenesis. We uncovered a unique expression pattern of LRP2 on ependymal cells exclusively in the lateral wall of the lateral ventricles where the stem cell niche is located. We also identified that loss of receptor expression in mutant mice results in a decline in proliferative capacity in the SEZ. Impaired proliferation of neuronal progenitor cells coincides with a distinct increase in BMP2/4 expression and enhanced activity of downstream signaling pathways, in line with a critical function for LRP2 as a negative modulator of BMP signaling, not only in embryonic but also in adult neurogenesis.

Journal of Cell Science

Results

LRP2 is expressed in ependymal cells of the stem cell niche

In the adult brain expression of LRP2 persists in the ventricular system (Zheng et al., 1994), but detailed information on the exact cellular location in the ventricles has been lacking. Using immunohistochemistry we detected LRP2 predominantly in the lateral ventricular system. Interestingly, the signal was restricted to the lateral and the immediate ventral-medial side of the lateral ventricle, the region of adult neurogenesis. By contrast, no LRP2 was detected on the medial side of the lateral ventricular wall (Fig. 1A). Within the lateral ventricular wall, the receptor was present exclusively on the apical surface of cells lining the ventricle but was not detectable deeper in the parenchyma in the subependymal zone (SEZ; Fig. 1A). To characterize cell types expressing the receptor we stained for S100β, an antigen highly expressed in ependymal cells. LRP2 immunoreactivity was detected close to the ependymal cells (Fig. 1B). However, in contrast to S100β, LRP2 was present exclusively in the ependyma adjacent to the stem cell niche (arrowheads in Fig. 1B), but not in S100β-positive (S100β+) ependyma at the medial side of the ventricular wall (asterisk in Fig. 1B). LRP2 was also coexpressed with sex-determining region Y-box protein 2 (SOX2) in cells of the ventricular epithelium but not the SEZ (Fig. 1C). No coexpression was observed with glial fibrillary acidic protein (GFAP; Fig. 1B). GFAP is expressed in astrocytes including B cell populations such as B1 cells, the putative stem cells of the SEZ (Mirzadeh et al., 2008).

To test whether LRP2 may also be expressed in apical extensions of B cells that reach the ventricular surface, we performed immunostaining of whole-mount preparations of the lateral ventricular surface (Fig. 2). Apical processes of SEZ B cells that reach the ventricular surface form the center of so called pinwheels, supracellular structures formed by clusters of ependymal cells (Mirzadeh et al., 2008). The pinwheel architecture of the ependyma can be visualized by staining for the cell surface marker β-catenin (Fig. 2A). In these preparations, LRP2 was detected on the apical surface of the ependymal cells but not in the extensions of B cells in the center of the pinwheel that were labeled by EGFP in a human GFAP-EGFP transgenic line (Nolte et al., 2001) (Fig. 2B).

Most ependymal cells have multiple cilia that contain CD133 (prominin 1). Although LRP2 immunoreactivity was seen on the apical surface of CD133+ cells, it did not colocalize with CD133, which suggested that the receptor is not present in the ciliary membrane (Fig. 2C; supplementary material Fig. S1). Rather, partial colocalization with γ-tubulin, which labels the basal body of the cilia, suggested that LRP2 was located in the apical membrane of the pericentriolar region (Fig. 2D; supplementary material Fig. S2).

In summary, LRP2 is expressed specifically in the lateral and ventral medial wall of the lateral ventricle, the site of adult neurogenesis. The receptor was detected on multiciliated S100β+, SOX2+ cells facing the ventricular wall, i.e. ependymal cells. By contrast, the receptor is absent from the apical processes of B cells extending into the ependymal layer.

LRP2 deficiency does not affect the structural integrity of the adult ventricular system

Mice genetically deficient for LRP2 are a useful tool to investigate the contribution of the receptor to ependymal function in the adult brain. Two different mouse models with *Lrp2* gene disruption have

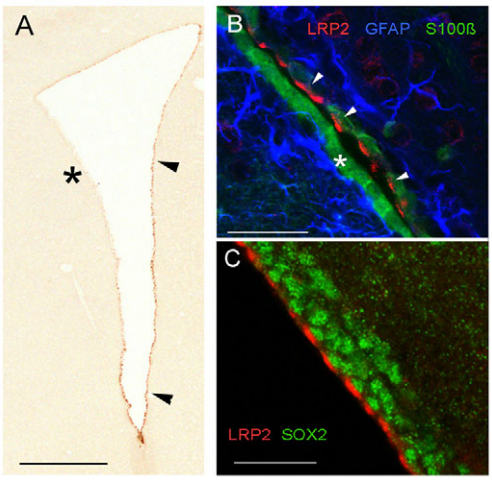

Fig. 1. Expression of LRP2 in the lateral wall of the lateral ventricles. (**A**) Immunodetection of LRP2 in the lateral ventricles of the adult mouse brain. The expression domain is restricted to the lateral and ventral medial side of the ventricular epithelium (arrowheads). No receptor expression is seen at the dorsal medial side (asterisk). (**B**) Immunohistological detection of LRP2 (red), S100β (green) and glial fibrillary acidic protein (GFAP; blue) in the lateral ventricles of the mouse brain. Note exclusive expression of LRP2 in the lateral (arrowheads) but not the medial side of the lateral ventricles (asterisk). (**C**) Expression of LRP2 (red) in SOX2+ cells (green) of the ventricular epithelium but not the subependymal zone. Scale bars: 500 µm in A; 50 µm in B and C.

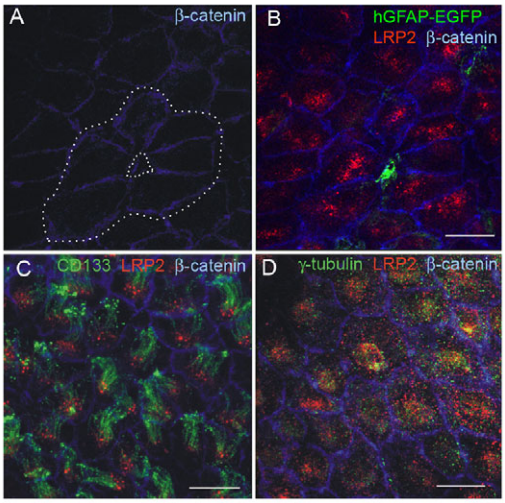

Fig. 2. Expression of LRP2 in ependymal cells of the lateral ventricles. Confocal images of the lateral wall of the lateral ventricle from whole-mount preparations. Staining for β-catenin (blue) was used to visualize the cell membranes in all panels. (**A**) Immunostaining for β-catenin reveals the pinwheel architecture of the ventricular surface of the lateral wall (one pinwheel indicated by dotted lines). (**B**) Immunostaining for EGFP (under control of the human glial fibrillary acidic protein promoter (hGFAP-EGFP; green), LRP2 (red), and β-catenin indicates LRP2 expression on the apical surface of ependymal cells forming the periphery of the pinwheel. No LRP2 is seen on the apical extensions of hGFAP-EGFP+ B cells. (**C**) LRP2 (red) is present in a speckled pattern on the apical surface of ependymal cells that have multiple cilia labeled for CD133 (green). No colocalization of the receptor is seen with CD133 in the membrane of the ciliary shaft. (**D**) Staining for γ-tubulin (green), LRP2 (red) and β-catenin (blue) shows partial colocalization of LRP2 and γ-tubulin in the ventricular epithelium. Scale bars: 100 µm.

been reported. Using homologous recombination in embryonic stem cells, we had previously generated mice carrying a receptor null allele (*Lrp2*$^{-/-}$) (Willnow et al., 1996). In addition, a mouse line with a missense mutation at amino acid position 2721 of the LRP2 polypeptide has been obtained in an ENU screen for models with altered brain cortex formation (line 267) (Zarbalis et al., 2004). The ENU mutation results in a premature stop codon in the sequence encoding the extracellular domain of LRP2 that abolishes receptor expression (Fig. 3A). Here, we have used the *Lrp2*$^{267/267}$ model as it has a higher rate of perinatal survival compared with the *Lrp2*$^{-/-}$ line. The difference in survival rate probably reflects distinct genetic backgrounds of *Lrp2*$^{267/267}$ (FVB/NJ×C57BL/6J) versus *Lrp2*$^{-/-}$ (129SvEmcTer×C57BL/6N) strains. All studies were performed in receptor-deficient *Lrp2*$^{267/267}$ animals and their gender-matched littermates. No phenotypic differences were observed between wild-type (*Lrp2*$^{+/+}$) and heterozygous (*Lrp2*$^{+/267}$) animals. Thus, both genotypes were used as reference and are collectively referred to as control animals (Ctr).

Because the consequence of LRP2 deficiency for structural integrity of the adult CNS has not, so far, been documented, we initially performed histo-anatomical analyses of the brains of *Lrp2*$^{267/267}$ animals. Adult mutant mice displayed subtle features of holoprosencephaly. Although the animals exhibited some degree of facial dysmorphology such as a shortened snout (Fig. 3B), their forebrains were divided into two hemispheres (Fig. 3C). Their olfactory bulbs (OB) appeared histologically normal (Fig. 3D). In line with a mild holoprosencephalic syndrome, the lumen of the ventricular system was partially enlarged (Fig. 3E), but no discernable differences were observed in the cortical layering of the brain (supplementary material Fig. S3). Also, the architecture of the ventricular epithelium appeared normal with the typical pinwheel arrangement of ependymal cells (Fig. 4). Moreover, the ultrastructure of the ependymal cell layer in the lateral ventricles of *Lrp2*$^{267/267}$ animals was undisturbed, as shown by immunostaining of whole-mount ventricular surface preparations for the cilia marker acetylated tubulin (Fig. 5A,B) and by scanning and transmission electron microscopy (Fig. 5C-H).

Proliferation is reduced in the SEZ but not the SGZ of LRP2-deficient mice

Defects in midline patterning during embryonic development did not grossly affect the neuroanatomy of the brain cortex or the ultrastructure of the lateral ventricles in adult LRP2 null mice. Thus, this mouse model was suitable for exploring the role of the receptor in the ventricular system of the adult brain. To test the consequence of LRP2 deficiency for adult neurogenesis, we labeled fast proliferating cells in the brains of 2- to 5-month old mice with a single intraperitoneal injection of BrdU. Twenty-four hours later, BrdU+ cells in the SEZ of control and *Lrp2* mutant mice were counted (Fig. 6A,B). There were 35% fewer fast proliferating cells in the SEZ of LRP2-deficient compared with control animals (Fig. 6E). This defect in proliferation appears in adulthood since evaluation of the proliferative capacity in the lateral ventricles in mice at postnatal day 10 did not show any difference between LRP2-deficient neonates and control littermates (supplementary material Fig. S4).

Cells born in the adult SEZ migrate to the OB to form interneurons in a path known as the rostral migratory stream (RMS). No qualitative differences were seen in the appearance of this stream, when BrdU+ cells were visualized in *Lrp2*$^{267/267}$ and control animals 4 days after BrdU application (supplementary material Fig. S5). A quantitative analysis of the total number of migratory BrdU+ cells was not performed in the RMS but in the OB. There were significantly fewer BrdU+ cells in the OB of *Lrp2*$^{267/267}$ mice compared with controls when evaluated 2 weeks after a single BrdU dose (Fig. 6C,E). This finding was in line with the overall decrease in cell proliferation in the SEZ of these animals. The lack of BrdU+ cells in the SEZ was not caused by increased apoptosis in receptor null mice as shown by TUNEL assay (supplementary material Fig. S6).

In contrast to the lateral wall of the lateral ventricle, LRP2 is not expressed in the hippocampus. Remarkably, the proliferative capacity of progenitors in the SGZ of the dentate gyrus of receptor-deficient mice was identical to that of control animals as documented by BrdU incorporation studies (Fig. 6D,E). This

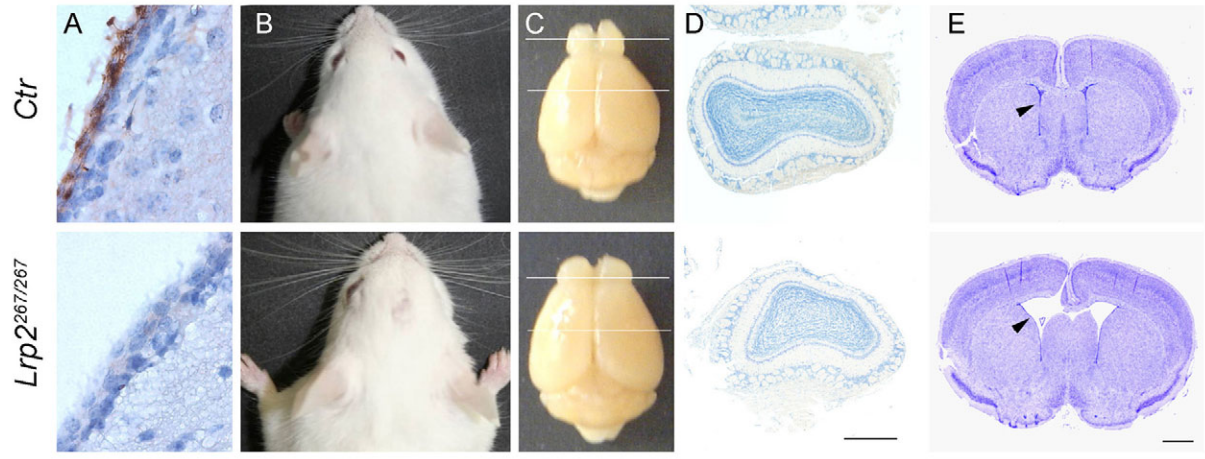

Fig. 3. Absence of LPR2 expression in the ventricular system of the *Lrp2*$^{267/267}$ mouse. (**A**) Expression of LRP2 in the lateral ventricles in *Lrp2*$^{+/+}$ control (Ctr) but not in *Lrp2*$^{267/267}$ mice as shown by immunohistochemistry. (**B**) Heads of adult mice indicating facial dysmorphology in the *Lrp2*$^{267/267}$ mouse compared with the control littermate. (**C**) Brains of control and *Lrp2*$^{267/267}$ animals indicating the plane of the sections in D and E. (**D**,**E**) Nissl-stained paraffin sections of olfactory bulbs (D) and forebrain hemispheres (E) in *Lrp2*$^{267/267}$ and littermate control mice. Arrowheads in E indicate an enlarged lumen of the ventricular system in the LRP2-deficient brain (lower panel). Scale bars: 500 μm.

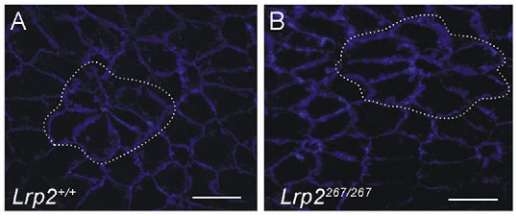

Fig. 4. Pinwheel architecture of the ventricular epithelium. Confocal images taken from the surface of whole mounts of the lateral wall of the lateral ventricle of *Lrp2*$^{+/+}$ and *Lrp2*$^{267/267}$ mice. All whole mounts were stained for β-catenin. Exemplary pinwheels are indicated in *Lrp2*$^{+/+}$ (**A**) and *Lrp2*$^{267/267}$ (**B**) preparations by dotted lines. Scale bars: 100 µm.

observation indicated a unique role for LRP2 in neurogenesis in ependymal cells as part of the neurogenic niche of the SEZ.

LRP2 deficiency impairs cell proliferation in the SEZ

In the SEZ, B cells give rise to transit-amplifying cells (C cells) that produce type A migratory neuroblasts, the immediate progenitors of newborn neurons. The reduction in numbers of BrdU+ cells in the SEZ of LRP2 null mice may reflect impairment in expansion and/or inappropriate differentiation of precursor and progenitor cells.

To identify which cell type was affected by receptor deficiency, we labeled the various populations of SEZ precursor cells for proteins characteristic for the respective cell population. Subsequently, we quantified the number of immunopositive cells or the mean fluorescence intensity in the SEZ. We found less GFAP (Fig. 7A,E), SOX2 (Fig. 7B,E), and Lewis X (LeX; Fig. 7C,E) in the SEZ of LRP2 null mice compared with controls. GFAP labels SEZ astrocytes (B cells) whereas SOX2 marks astrocytes as well as other SEZ progenitors. LeX, a carbohydrate expressed in SEZ pluripotent neuronal stem cells, is described as one of the most specific markers for B cells contributing to the stem cell pool (Capela and Temple, 2002). Conversely, distal-less homeobox 2 (DLX2, Fig. 8A) is expressed in C cells and A cells, while doublecortin (DCX; Fig. 8B) and polysialic acid neural cell adhesion molecule (PSA-NCAM; Fig. 8C) are diagnostic of A cells. Notably, there were substantially fewer DLX2, DCX and PSA-NCAM-positive cells in *Lrp2* mutants (Fig. 8D).

To further examine the reduction in various SEZ cell types, we crossed the LRP2-deficient mouse model with a reporter line expressing GFP under control of the neural precursor cell-specific nestin promoter (nestin-GFP; B and C cells). The signal for GFP in the SEZ was significantly reduced in *nestin-GFP;Lrp2*$^{267/267}$ compared with *nestin-GFP;Lrp2*$^{+/+}$ animals (Fig. 7D,E). In contrast to the situation in the SEZ, the number of nestin-GFP+ and PSA-NCAM+ precursor cells was similar in the SGZ of receptor-deficient mice and littermate controls (supplementary material Fig. S7).

To evaluate the impact of LRP2 deficiency on gliogenesis we analyzed the expression of the transcription factor OLIG2 in the lateral wall of the lateral ventricle. OLIG2 is specifically expressed in gliogenic progenitors in the adult SEZ (Colak et al., 2008; Hack et al., 2005). Counts of OLIG2+ cells did not reveal any significant difference between LRP2-deficient and control mice (supplementary material Fig. S8A). Undisturbed gliogenesis was also confirmed by staining for platelet-derived growth factor receptor α (supplementary material Fig. S9) that is expressed in a subset of subependymal zone astrocytes implicated in genesis

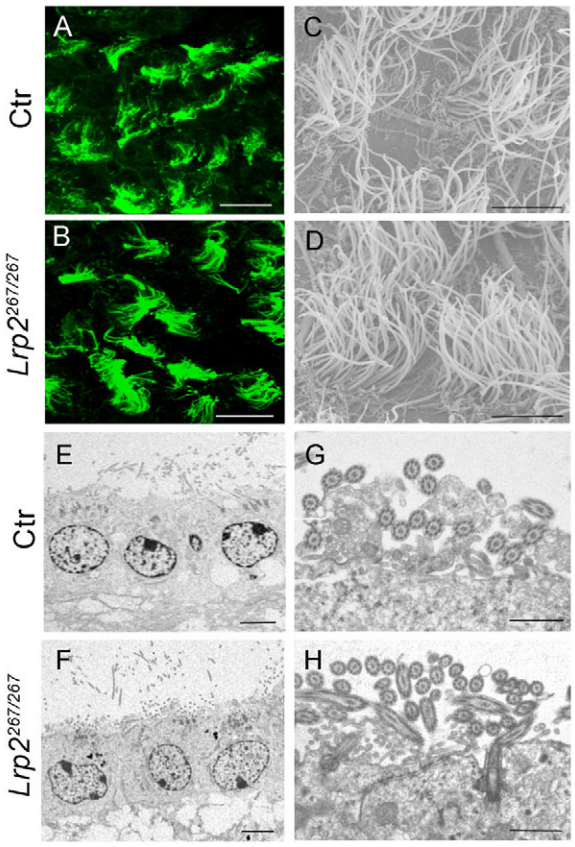

Fig. 5. Immunohistological analysis and electron microscopy of the ventricular zone in control and LRP2-deficient adult mice. (**A**,**B**) Confocal images taken from the surface of whole-mounts of the lateral wall of the lateral ventricle of control (Ctr) and LRP2-deficient (*Lrp2*$^{267/267}$) mice stained for the cilia marker acetylated tubulin. (**C**,**D**) Scanning electron microscopy of the apical surface of the lateral ventricles in mice of the indicated genotypes. No obvious anomalies are seen in the appearance of the multi-ciliated apical cell surface of the ependyma in receptor-deficient (D) compared with control (C) mice. (**E-H**) Transmission electron microscopy of the ventricular zone in mice of the indicated genotypes. The morphology of the ependymal cells (E,F) and the molecular architecture of their cilia (G,H) appear indistinguishable in Ctr and *Lrp2*$^{267/267}$ mice. Scale bars: 100 µm in A,B; 10 µm in C,D; 5 µm in E,F; 1 µm in G,H.

of the oligodendroglial lineage (Merkle and Alvarez-Buylla, 2006).

So far, our findings indicated impaired cell proliferation in the SEZ of LRP2 null mice that equally affected the neural precursor cell population and their immediate progeny. This interpretation was confirmed by quantification of BrdU+ cells that expressed DLX2 (C cells) or DCX with or without DLX2 (A cells, neuroblasts; Fig. 9). Although the total number of BrdU+ cells was reduced in the receptor-deficient line, the proportion of individual BrdU+ C and A cell populations was unchanged in the SEZ of LRP2 null mice compared with littermate controls, suggesting that LRP2 deficiency leads to a reduction in the C cell pool and reduced proliferative activity rather than a major change in cell fate of the progenitors, e.g. towards the oligodendroglial lineage.

Loss of LRP2 increases BMP2/4 signaling in the SEZ

In the embryonic neuroepithelium, LRP2 has been proposed to act as an endocytic receptor for BMP4 (Spoelgen et al., 2005). LRP2-

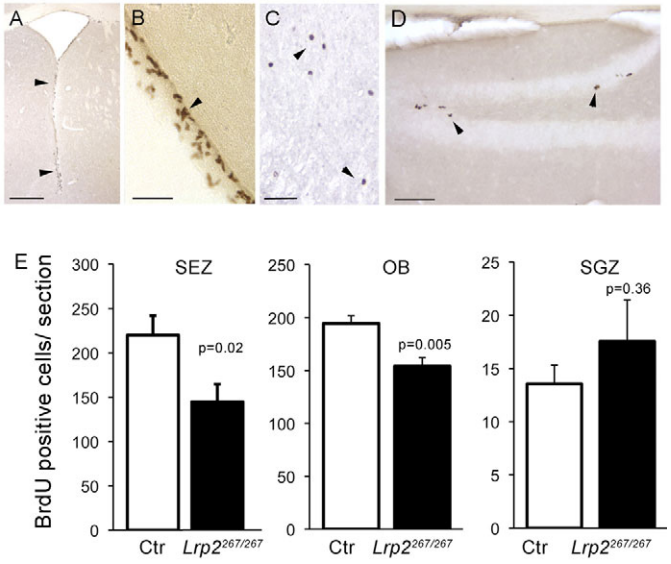

Fig. 6. Immunohistological detection and quantification of BrdU+ cells in subependymal zone, olfactory bulb and subgranular zone of LRP2-deficient and control mice. (**A-D**) Immunohistological detection of BrdU+ cells in the subependymal zone (A,B), the olfactory bulbs (C) and the subgranular zone (D) of LRP2-deficient mice. Scale bars: 500 µm in A; 50 µm in B, C; 100 µm in D. (**E**) Quantification of BrdU+ cells in the subependymal zone (SEZ) at 24 hours, in the olfactory bulb (OB) at 2 weeks, and in the subgranular zone (SGZ) at 24 hours after BrdU injection. The numbers of BrdU+ cells are indicated as total cell counts per section of control animals (Ctr) and *Lrp2*$^{267/267}$ mutants. Mean values ± standard error of the mean were determined by counting the number of BrdU+ cells on a total of 12 representative sections from each animal (six or seven animals per genotype).

mediated clearance of BMP4 downregulates this signaling pathway in the forebrain and ensures neurogenesis from the ventral region of the neural tube. Given the established role of BMP4 as a negative modulator of neurogenesis in the SEZ, we wondered whether LRP2 might have a similar function in the adult brain and whether an increase in BMP signaling may underlie the neurogenesis defect in *Lrp2*$^{267/267}$ mice. To address this question, we analyzed the BMP signaling pathway in the lateral ventricles of control and LRP2-deficient animals using immunohistochemistry. We detected a distinct increase in the expression levels of BMP2/4 in the SEZ of *Lrp2*$^{267/267}$ compared with control mice (Fig. 10A). Enhanced activity of the BMP signaling cascade was substantiated by staining for phosphorylated forms of SMAD1/5/8 proteins, intracellular effectors of BMP signaling (Fig. 10B). Quantification of stained cell nuclei uncovered a fourfold increase in phospho-SMAD1/5/8-positive cells in the SEZ of LRP2-deficient compared with control mice (Fig. 10D). Inhibitor of DNA binding 3 (ID3) is a downstream target of BMP4 signaling (Miyazono and Miyazawa, 2002). Consistent with an aberrant increase in this morphogen pathway in LRP2-deficient mice, immunohistological signals for ID3 were also distinctly stronger in the SEZ of these animals (Fig. 10C). Quantification of ID3+ cells revealed that there were twice as many in the SEZ of *Lrp2*$^{267/267}$ mice compared with littermate controls (Fig. 10D).

Finally to characterize the phospho-SMAD1/5/8+ and ID3+ cells in more detail, we performed co-staining experiments using antibodies against phospho-SMAD1/5/8 or ID3 with antibodies against markers for the different SEZ cell types. Strikingly, a significantly higher proportion of nestin-GFP+ and SOX2+ cells in the SEZ of LRP2-deficient mice were positive for phospho-SMAD1/5/8 or ID3 compared with controls (Fig. 11). By contrast, there were fewer DLX2+ cells (C cells) that were also positive for ID3 in both control and mutant mice and there was no statistically significant difference between genotypes (Fig. 12). These results suggest that it is predominantly the nestin+ and SOX2+ cell population (B cells) that responds to ectopic and enhanced BMP4 signaling in the SEZ.

Discussion

Our studies demonstrate an essential role for LRP2, an endocytic receptor in ependymal cells, as a negative modulator of BMP

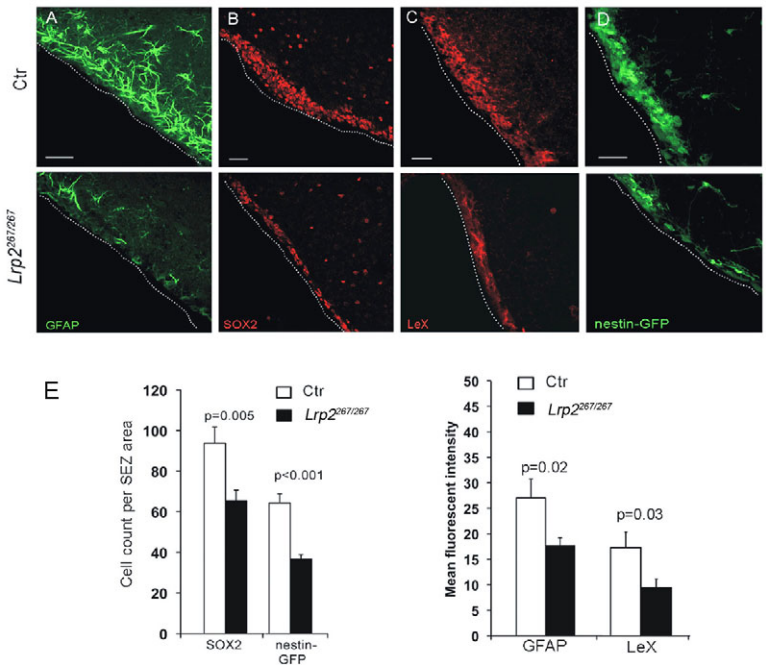

Fig. 7. Immunohistological detection and quantification of neuronal precursor cell population in *Lrp2*$^{267/267}$ and control mice. (**A-D**) Immunodetection of cell populations in the subependymal zone of control (Ctr) and *Lrp2*$^{267/267}$ mice positive for glial fibrillary acidic protein (GFAP; A), sex determining region Y-box protein 2 (SOX2; B), Lewis X (LeX; C) and nestin-green fluorescent protein (nestin-GFP; D). The images indicate fewer cells positive for all four markers in the subependymal zone of LRP2-deficient mice. The apical surface of the ependyma is indicated by dotted lines. Scale bars: 50 µm. (**E**) Cells immunopositive for SOX2 and nestin-GFP in the subependymal zone (SEZ) of *Lrp2*$^{267/267}$ and control mice (Ctr) were counted. GFAP and LeX in the SEZ of *Lrp2*$^{267/267}$ and control mice were scored as mean fluorescence intensities. Four histological sections from each individual mouse (four or five mice in each group) were scored. Statistical significance of differences was determined using Student's *t*-test.

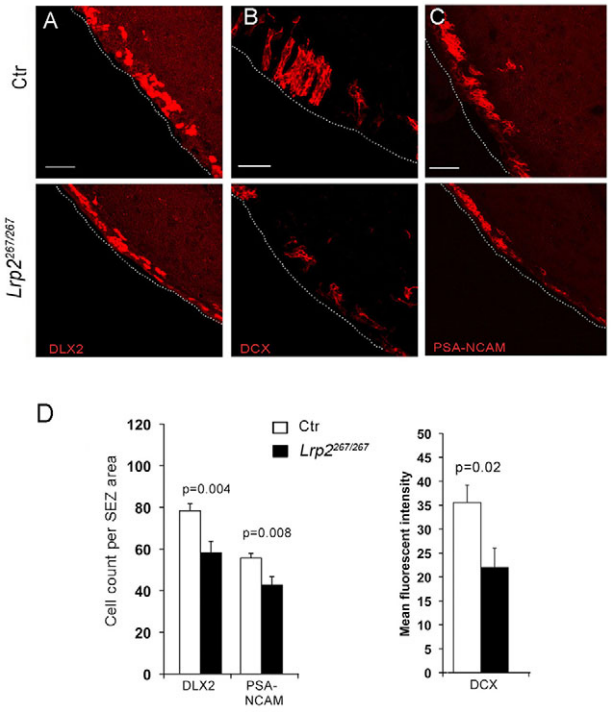

Fig. 8. Immunohistological detection and quantification of C cell and A cell populations in the subependymal zone of *Lrp2*$^{267/267}$ and control mice. (**A-C**) Immunodetection of cell populations in the subependymal zone of control (Ctr) and *Lrp2*$^{267/267}$ mice positive for distal-less homeobox 2 (DLX2; A), doublecortin (DCX; B), and polysialic acid-neural cell adhesion molecule (PSA-NCAM; C). The images show fewer numbers of cells positive for all three markers in the subependymal zone of LRP2-deficient mice. The apical surface of the ependyma is indicated by dotted lines. Scale bars: 50 µm. (**D**) Cells immunopositive for DLX2 and PSA-NCAM in the subependymal zone (SEZ) of *Lrp2*$^{267/267}$ and control mice (Ctr) were counted. Signals for DCX in the SEZ of *Lrp2*$^{267/267}$ and control mice were scored as mean fluorescence intensity. Four histological sections from each individual mouse (four or five mice in each group) were scored. Statistical significance of differences between control and *Lrp2* mutant animals was determined using Student's *t*-test.

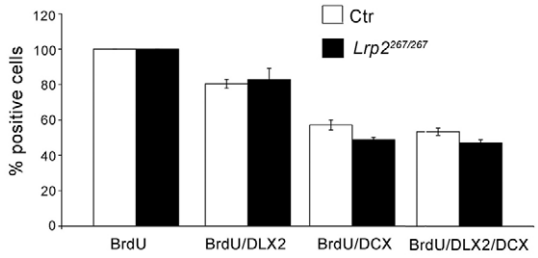

Fig. 9. Quantification of BrdU+ C cell and A cell populations in the subependymal zone. The percentage of BrdU+ cells in the subependymal zone co-stained with the indicated cellular markers was quantified. A total of 300 BrdU+ cells were counted for each animal and set at 100% (six animals per genotype). DLX2, distal-less homeobox 2; DCX, doublecortin.

signaling in the adult stem cell niche. Loss of receptor activity results in abnormally increased activity of the BMP2/4 pathway in the SEZ. As a consequence, progenitor proliferation is suppressed and neurogenic output reduced from this niche. Neurogenesis in the SGZ, the second germinal niche in the adult mammalian brain, is not affected by receptor deficiency, supporting a distinct role of the ependyma (and LRP2) in this signaling pathway that is unique to the SEZ.

Previously, the significance of the ependyma has mainly been discussed in terms of a barrier function, protecting the brain from noxious substances that accumulate in the cerebrospinal fluid (reviewed by Del Bigio, 1995). An exciting new aspect of ependymal function was recognized when it was shown that proliferation of neural stem cells persists in the SEZ of the adult brain, a region that is intimately linked to the lateral ventricles (Lois and Alvarez-Buylla, 1993; Morshead et al., 1994; Reynolds and Weiss, 1992). How ependymal cells contribute to neurogenic processes has been a matter of debate (see Chojnacki et al., 2009). It was first suggested that ependymal cells act as neuronal precursor cells under normal physiological conditions (Johansson et al., 1999). This idea was later largely abandoned, as a role of astrocytes as the sole precursors in the SEZ was favored. However, recent reports provide new evidence that ependymal cells may act as precursor cells after brain injury (Carlen et al., 2009).

Another hypothesis proposes that rather than acting as stem cells, ependymal cells contribute to the microenvironment in the stem cell niche, which is critical for neurogenesis (Colak et al., 2008; Lim et al., 2000). This hypothesis is supported by findings that factors in the stem cell niche provide instructive signals for neurogenesis. Thus, progenitors from the SEZ grafted into other SEZs produce large numbers of neurons, but fail to do so when transplanted into non-neurogenic brain regions (Doetsch and Alvarez-Buylla, 1996; Lois and Alvarez-Buylla, 1994). Inactivation of genes expressed in the ependyma such as *Numb* (Kuo et al., 2006) and *Sox2* (Ferri et al., 2004) impairs adult neurogenesis. However, both genes are also expressed in SEZ progenitors and no firm conclusion could be drawn about whether loss of activity in the ependyma and/or in the SEZ underlies the observed neurogenic defects. The functional elucidation of an ependymal cell surface receptor, LRP2, that is required for proper neurogenesis to occur from SEZ precursor cells now provides genetic proof for a critical contribution of the ependyma to adult neurogenesis.

It is particularly fascinating that unlike other proteins expressed throughout the ependyma (e.g. S100β, vimentin, mCD24) (Mirzadeh et al., 2008), LRP2 is not uniformly distributed throughout the ventricular system. Rather, expression is highest in the lateral ventricles where it is seen exclusively in the ependyma adjacent to the stem cell niche (Fig. 1A,B). Within the ventricular epithelium of the stem cell niche LRP2 localizes to the apical surface of multiciliated ependymal cells forming the periphery of the pinwheel structure but it is absent from the apical surface of GFAP+ B cells (Fig. 2B). Thus, LRP2 represents a unique marker that functionally discriminates ependymal cells in the neurogenic zone from ependyma elsewhere in the lateral ventricles.

Neurogenesis in the SEZ is impaired in mice genetically deficient for LRP2 (Fig. 6). Signals for nestin-GFP, SOX2, GFAP and LeX all are reduced in the SEZ of LRP2-deficient mice (Fig. 7) suggesting a negative impact of receptor deficiency on the B cell pool. Depletion of the B1 cell pool is expected to lead to a reduced number of progenitor cells. This assumption was confirmed by an overall decrease in markers for transit-amplifying progenitors and the neuroblasts (DLX2, DCX and PSA-NCAM; Fig. 8). Neurogenesis in the SGZ is not affected, demonstrating confinement of the stem cell defect to brain regions that normally express

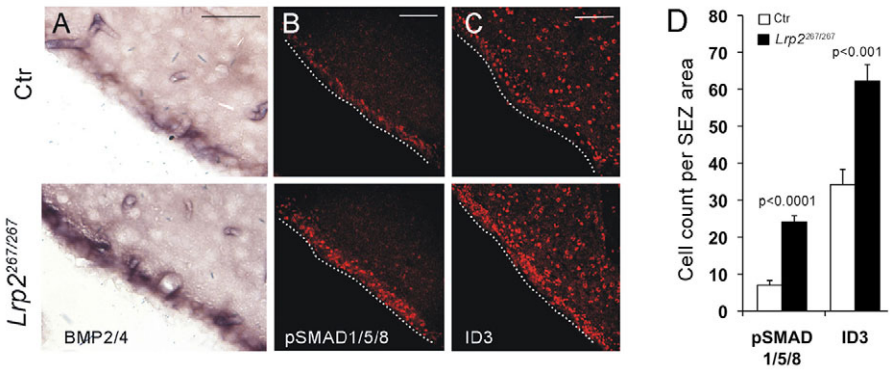

Fig. 10. BMP signaling pathway in the subependymal zone. (**A-C**) Immunohistological analysis detects stronger signals for bone morphogenetic protein 2/4 (BMP2/4; A), phosphorylated variants of similar to mothers against decapentaplegic homolog (pSMAD1/5/8; B), and of inhibitor of DNA binding 3 (ID3; C) in the subependymal zone of LRP2-deficient mice compared with control littermates (Ctr). Scale bars: 50 µm in A; 100 µm in B, C. (**D**) Quantification of the cells positive for phospho (p) SMAD1/5/8 and ID3 in the subependymal zone (SEZ) of *Lrp2*$^{267/267}$ and control mice as shown in B and C. A total of four histological sections from four to seven mice in each group were quantified. Statistical significance of differences between control and *Lrp2* mutant animals were determined using Student's *t*-test.

LRP2. In contrast to the reduction in transit-amplifying progenitors and neuroblasts we failed to detect a difference in oligodendrocyte precursor cell numbers in the receptor-null model (supplementary material Figs S8 and S9). Thus, LRP2 deficiency does not affect proliferation of this subset of glial progenitors.

Other than induction of apoptosis (supplementary material Fig. S6), several mechanisms might cause a decrease or re-specification of the progenitor cell population in LRP2-deficient mice. For example, impaired ability of the stem cells to self-renew (as in mice lacking the orphan receptor tailless) (Liu et al., 2008), changes in cell cycle length regulation (as in *p21* mutant mice) (Doetsch et al., 2002; Kippin et al., 2005) or redirection of cell fate specification (as in mice lacking SMAD4) (Colak et al., 2008) have all been shown to affect the neural precursor pool. Whatever the exact mechanism might be, alterations in such cell intrinsic pathways in the SEZ are probably downstream of a primary defect in the instructive capacity of ependymal cells caused by LRP2 deficiency.

One of the major instructive signals in the SEZ is provided by BMPs, members of the transforming growth factor β superfamily. Both BMP4 and 7 and their receptors are widely expressed by neurons and astrocytes throughout the adult CNS (Mikawa et al., 2006; Peretto et al., 2004). Within the neurogenic niche of the SEZ phospho-SMAD1/5/8 are restricted to stem cells and transit-amplifying progenitors (Colak et al., 2008). Expression of BMPs in the neurogenic regions of the adult brain seemed counter-intuitive given their anti-proliferative potential. Indeed, overexpression of BMP7 by adenoviral-mediated gene transfer into the ependyma decreases SEZ proliferation and prevents further neurogenesis (Lim et al., 2000). Thus, raising the levels of BMP interferes with proliferation and survival of neurogenic progenitors, highlighting the importance of noggin, a potent antagonist of BMP signaling, secreted by ependymal cells. Indeed, BMP levels are crucial, because their further reduction by infusing noggin into the ventricle (Lim et al., 2000) or conditional inactivation of *Smad4* in GLAST+ adult neural stem cells resulted in severely reduced neurogenesis due to the ectopic upregulation of the transcription factor OLIG2, directing the progenitors towards oligodendrogliogenesis (Colak et al., 2008).

Taken together, the findings discussed above suggest an important role for the ependyma in modulating BMP signaling, thereby providing the instructive milieu for neurogenesis in the SEZ. This hypothesis receives convincing support from our work showing that ependymal cells express LRP2, an endocytic receptor

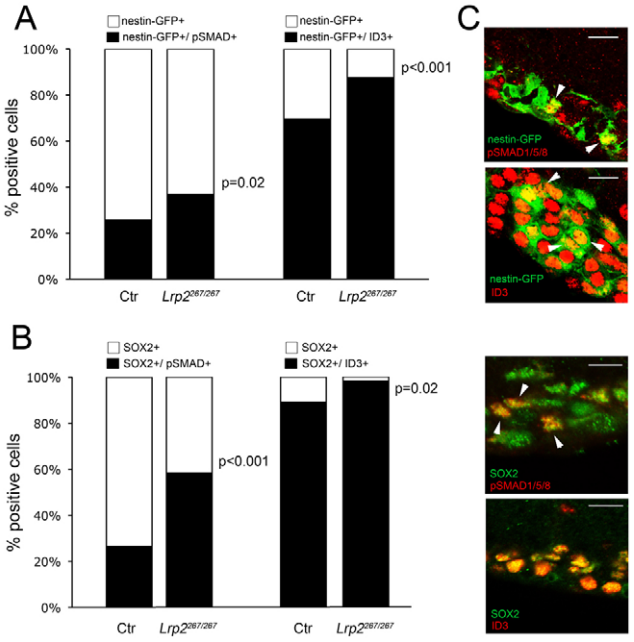

Fig. 11. Analysis of the BMP signaling pathway in nestin+ and SOX2+ cells in the subependymal zone. (**A**,**B**) The percentage of nestin-GFP+ (A) and of SOX2+ (B) cells in the subependymal zone co-stained with either phospho- (p) SMAD1/5/8 or ID3 was quantified. A total of 300 nestin-GFP+ or SOX2+ cells were counted for each experiment and set at 100% (white bars) to adjust for the difference in total cell count between genotypes. The percentage overlap in phospho-SMAD1/5/8 or ID3signal in both genotypes is given (black bars). Statistically significant increases in nestin-GFP+ and SOX2+ cells that respond to BMP signaling as documented by phospho-SMAD1/5/8 and ID3 signals are seen in *Lrp2*$^{267/267}$ mice. A total of 16 histological sections from three to five animals in each group were evaluated. Statistical significance of differences was determined using Student's *t*-test. (**C**) Immunohistological micrographs of the indicated double labeling experiments. Scale bars: 13 µm.

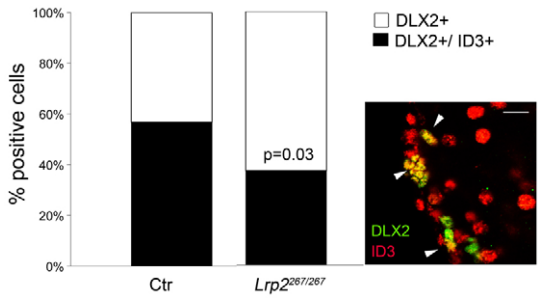

Fig. 12. Analysis of the BMP signaling pathway in the C cell population of the subependymal zone. The percentage of DLX2+ cells in the subependymal zone co-stained with ID3 were quantified. A total of 300 DLX2+ cells were counted for each experiment and set at 100% (white bars) to adjust for differences in total cell count between genotypes. The percentage of cells also positive for ID3 signal in both genotypes is given (black bars). A total of 16 histological sections from three to five animals in each group were evaluated. Statistical significance was determined using Student's *t*-test. An immunohistological micrograph of the double labeling experiment is also shown. Scale bar: 17 µm.

for BMPs. LRP2 has been shown to bind BMP4 (but not BMP5) in vitro (Spoelgen et al., 2005). Binding results in cellular uptake and catabolism of BMP4, conceivably reducing the amount of morphogen available to activate its cognate BMP receptors (Spoelgen et al., 2005). Inactivation of the receptor pathway in the mouse results in enhanced BMP signaling and in impairment of neurogenesis in the embryonic neural tube (Spoelgen et al., 2005). The data presented here indicate that the function of LRP2, as a negative regulator of BMP signaling, is conserved in the adult brain where lack of the receptor causes aberrant increase in BMP signaling in the SEZ (Fig. 10).

Interestingly, enhanced BMP signaling as reflected by increased phospho-SMAD1/5/8 and ID3 signals mainly affects the nestin+ and SOX2+ cell population in *Lrp2*$^{267/2767}$ mice. When adjusted for the overall decrease in the pool of nestin+ and SOX2+ cells in the SEZ of mutant mice, a significantly larger overlap with markers of the BMP signaling pathway was observed (Fig. 11). By contrast, no specific rise in numbers of DLX2-ID3 double-positive C cell types was seen (Fig. 12). These results demonstrate that a higher share of type B cells in mutant mice than in the controls remain BMP-responsive and therefore might be impaired in their self-renewal capacity and/or in their specification and differentiation towards the neurogenic lineage.

Ultimately, enhanced BMP signals as a consequence of LRP2 deficiency coincide with a significant decrease in progenitor (C cell) proliferation, substantiating the crucial role of the ependyma in reducing BMP activity to promote SEZ neurogenesis. This model is particularly exciting as ependymal cells are unique to one of the major stem cell niches, the SEZ, and are not part of the SGZ in the dentate gyrus. Indeed, the function of LRP2 thereby highlights a key difference between the two stem cell niches that produce distinct types of neurons. Further detailed characterization of the LRP2 pathway will help in elucidating the unique processes that govern neurogenesis in these neurogenic zones.

Materials and Methods

Mouse models

An LRP2-deficient mouse strain was identified in an ENU screen for mutations that impair morphogenesis of the brain cortex. In line 267 (*Lrp2*$^{267/267}$), a T to A transition results in a stop codon at amino acid position 2721 of the LRP2 polypeptide abolishing receptor expression (Zarbalis et al., 2004). A mouse line carrying a GFP transgene driven by the rat nestin promoter (nestin-GFP) was generously provided by M. Yamaguchi, University of Tokyo (Yamaguchi et al., 2000). A mouse model expressing EGFP under the control of the human GFAP promoter was obtained from H. Kettenmann, MDC Berlin (Nolte et al., 2001). All comparative analyses were performed in LRP2 null mice and their respective gender-matched littermate controls at 2-5 months of age.

Immunohistochemical analysis

Brain tissues were fixed in 4% paraformaldehyde in phosphate-buffered saline (PBS) overnight, followed by routine paraffin embedding and sectioning at 7-15 µm thickness (Fig. 1A, Fig. 3A,D-E, Fig. 6C, Fig 10A; supplementary material Fig. S3). Alternatively, fixed brain tissues were infiltrated with 30% sucrose in PBS for 48 hours. Thereafter, 40 µm free-floating sections were cut and stored in cryoprotectant at –20°C until further use (remaining figures unless stated otherwise). Standard immunohistochemical analysis was carried out by incubation of tissue sections with primary antibodies at the following dilutions: rabbit anti-megalin antiserum 612 (1:1000; kindly provided by J. Herz, UTSW Medical Center, Dallas, USA), mouse anti-S100β (1:1000; Sigma), mouse anti-LeX/CD15 (1:500, BD Biosciences), rabbit anti-PDGF receptor α (1:700; Santa Cruz), rabbit anti-S100β (1:2500; Swant), rat anti-prominin 1 (1:100; Ebioscience), rabbit anti-SOX2 (1:200; Chemicon), guinea pig anti-GFAP (1:1000; Advanced Immunochemicals), rabbit anti-GFP (1:400; Abcam), goat anti-DCX (1:200; Santa Cruz Biotechnology), mouse anti-PSA-NCAM (1:400; Chemicon), goat anti-BMP2/4 (1:100; Fitzgerald), rabbit anti-phospho-SMAD1/5/8 (1:500; Cell Signaling Technologies), guinea pig anti-DLX2 (1:200), rabbit anti-ID3 (1:100; Abcam) rabbit anti-Tbr1 (1:1000; Chemicon), rat anti-Ctip2 (1:200; Abcam), rabbit anti-Sox5 (1:20; Santa Cruz), or rabbit anti-FoxP2 (1:200; Abcam). Bound primary antibodies were visualized using secondary antisera conjugated with Alexa Fluor 488, 555, 546, 633, 647 (1:250; Invitrogen), FITC, TRITC, Rhodamin RedX, Cy5, Biotin-SP (1:250; Jackson Immuno Research), fluorescent conjugates of streptavidin (Invitrogen) or tyramide signal amplification kit (PerkinElmer). For double labeling experiments, the incubation with primary antibodies was performed sequentially. Apoptosis was determined on histological sections using the TUNEL assay according to manufacturer's recommendations (APO-BrdU TUNEL assay kit; Invitrogen). Immunofluorescence intensities were quantified on confocal multi-spectral laser scanning microscopes.

Electron microscopy

Samples of the lateral ventricles were dissected from adult mouse brains, fixed in 2.5% PBS-buffered glutaraldehyde, dehydrated in alcohol, osmicated, dried in a critical-point apparatus, coated with carbon, and examined in a Zeiss scanning electron microscope. For transmission EM, the tissues were fixed in 1% glutaraldehyde in PBS, postfixed in 1% OsO_4 (in sodium cacodylate buffer), stained en bloc in saturated uranyl acetate, dehydrated in graded ethanol and embedded in Epon. Sections were cut with a Leica Ultramicrotome UCT, stained with uranyl acetate and lead citrate, and examined in a FEI 100 CM electron microscope.

BrdU labeling experiments

To label proliferating cells in adult or postnatal brains, BrdU (Sigma) was injected intraperitoneally at 50 mg/kg body mass once, and the animals sacrificed 24 hours (SEZ, SGZ, P10), 4 days (RMS) or 2 weeks (OB) later. For quantification of BrdU-positive cells in the adult brain, free-floating sections were treated with 2 M HCl at 40°C for 45 minutes and neutralized by washing in 0.1 M sodium borate buffer (pH 8.5) for 10 minutes. Sections were blocked in 6% donkey serum in Tris-buffered saline plus 0.3% Triton X-100 for 1 hour. Then, sections were incubated with rat anti-BrdU antibody (1:500; AbD Serotec), followed by donkey anti-rat biotin SP antibody (1:250; Jackson Immuno Research) for 2 hours, and ABC-Elite reagent (PK-6100; Vector Labs) for 1 hour. Color reaction was performed using Ni-diamino benzidine. The number of labeled cells in the various brain regions was counted on 12 histological sections of each brain (×20 objective) that covered the entire area of the lateral ventricular system and the hippocampus, from the corpus callosum in the rostral to the cerebellum in the caudal region. For brains at postnatal day 10, BrdU+ cells in the SVZ were evaluated using Cell-F microscope software (Soft Imagining System). The SVZ was defined as a region of interest (ROI) and the average grey value corresponding to immunostained nuclei recorded on five to ten SVZ coronal sections in binary color image mode. Statistical significance of data was determined using Student's *t*-test.

We are indebted to M. Schmeisser, P. Schrade, I. B. Kristoffersen, and K. Kampf for expert technical assistance, and to G. Lewin for critical reading of the manuscript. Studies were funded in part by the DFG, SFB 665 (to T.E.W. and A.H.).

Supplementary material available online at
http://jcs.biologists.org/cgi/content/full/123/11/1922/DC1

References

Assemat, E., Chatelet, F., Chandellier, J., Commo, F., Cases, O., Verroust, P. and Kozyraki, R. (2005). Overlapping expression patterns of the multiligand endocytic receptors cubilin and megalin in the CNS, sensory organs and developing epithelia of the rodent embryo. *Gene Expr. Patterns* **6**, 69-78.

Balordi, F. and Fishell, G. (2007). Hedgehog signaling in the subventricular zone is required for both the maintenance of stem cells and the migration of newborn neurons. *J. Neurosci.* **27**, 5936-5947.

Bertrand, N. and Dahmane, N. (2006). Sonic hedgehog signaling in forebrain development and its interactions with pathways that modify its effects. *Trends Cell. Biol.* **16**, 597-605.

Capela, A. and Temple, S. (2002). LeX/ssea-1 is expressed by adult mouse CNS stem cells, identifying them as nonependymal. *Neuron* **35**, 865-875.

Carlen, M., Meletis, K., Goritz, C., Darsalia, V., Evergren, E., Tanigaki, K., Amendola, M., Barnabe-Heider, F., Yeung, M. S., Naldini, L. et al. (2009). Forebrain ependymal cells are Notch-dependent and generate neuroblasts and astrocytes after stroke. *Nat. Neurosci.* **12**, 259-267.

Chojnacki, A. K., Mak, G. K. and Weiss, S. (2009). Identity crisis for adult periventricular neural stem cells: subventricular zone astrocytes, ependymal cells or both? *Nat. Rev. Neurosci.* **10**, 153-163.

Colak, D., Mori, T., Brill, M. S., Pfeifer, A., Falk, S., Deng, C., Monteiro, R., Mummery, C., Sommer, L. and Gotz, M. (2008). Adult neurogenesis requires Smad4-mediated bone morphogenic protein signaling in stem cells. *J. Neurosci.* **28**, 434-446.

Del Bigio, M. R. (1995). The ependyma: a protective barrier between brain and cerebrospinal fluid. *Glia* **14**, 1-13.

Doetsch, F. and Alvarez-Buylla, A. (1996). Network of tangential pathways for neuronal migration in adult mammalian brain. *Proc. Natl. Acad. Sci. USA* **93**, 14895-14900.

Doetsch, F., Verdugo, J. M., Caille, I., Alvarez-Buylla, A., Chao, M. V. and Casaccia-Bonnefil, P. (2002). Lack of the cell-cycle inhibitor p27Kip1 results in selective increase of transit-amplifying cells for adult neurogenesis. *J. Neurosci.* **22**, 2255-2264.

Ehninger, D. and Kempermann, G. (2008). Neurogenesis in the adult hippocampus. *Cell Tissue Res.* **331**, 243-250.

Ferri, A. L., Cavallaro, M., Braida, D., Di Cristofano, A., Canta, A., Vezzani, A., Ottolenghi, S., Pandolfi, P. P., Sala, M., DeBiasi, S. et al. (2004). Sox2 deficiency causes neurodegeneration and impaired neurogenesis in the adult mouse brain. *Development* **131**, 3805-3819.

Fuccillo, M., Joyner, A. L. and Fishell, G. (2006). Morphogen to mitogen: the multiple roles of hedgehog signalling in vertebrate neural development. *Nat. Rev. Neurosci.* **7**, 772-783.

Hack, M. A., Saghatelyan, A., de Chevigny, A., Pfeifer, A., Ashery-Padan, R., Lledo, P. M. and Gotz, M. (2005). Neuronal fate determinants of adult olfactory bulb neurogenesis. *Nat. Neurosci.* **8**, 865-872.

Johansson, C. B., Momma, S., Clarke, D. L., Risling, M., Lendahl, U. and Frisen, J. (1999). Identification of a neural stem cell in the adult mammalian central nervous system. *Cell* **96**, 25-34.

Kippin, T. E., Martens, D. J. and van der Kooy, D. (2005). p21 loss compromises the relative quiescence of forebrain stem cell proliferation leading to exhaustion of their proliferation capacity. *Genes Dev.* **19**, 756-767.

Kriegstein, A. and Alvarez-Buylla, A. (2009). The glial nature of embryonic and adult neural stem cells. *Annu. Rev. Neurosci.* **32**, 149-184.

Kuo, C. T., Mirzadeh, Z., Soriano-Navarro, M., Rasin, M., Wang, D., Shen, J., Sestan, N., Garcia-Verdugo, J., Alvarez-Buylla, A., Jan, L. Y. et al. (2006). Postnatal deletion of Numb/Numblike reveals repair and remodeling capacity in the subventricular neurogenic niche. *Cell* **127**, 1253-1264.

Lim, D. A., Tramontin, A. D., Trevejo, J. M., Herrera, D. G., Garcia-Verdugo, J. M. and Alvarez-Buylla, A. (2000). Noggin antagonizes BMP signaling to create a niche for adult neurogenesis. *Neuron* **28**, 713-726.

Liu, H. K., Belz, T., Bock, D., Takacs, A., Wu, H., Lichter, P., Chai, M. and Schutz, G. (2008). The nuclear receptor tailless is required for neurogenesis in the adult subventricular zone. *Genes Dev.* **22**, 2473-2478.

Lledo, P. M., Merkle, F. T. and Alvarez-Buylla, A. (2008). Origin and function of olfactory bulb interneuron diversity. *Trends Neurosci.* **31**, 392-400.

Lois, C. and Alvarez-Buylla, A. (1993). Proliferating subventricular zone cells in the adult mammalian forebrain can differentiate into neurons and glia. *Proc. Natl. Acad. Sci. USA* **90**, 2074-2077.

Lois, C. and Alvarez-Buylla, A. (1994). Long-distance neuronal migration in the adult mammalian brain. *Science* **264**, 1145-1148.

Machold, R., Hayashi, S., Rutlin, M., Muzumdar, M. D., Nery, S., Corbin, J. G., Gritli-Linde, A., Dellovade, T., Porter, J. A., Rubin, L. L. et al. (2003). Sonic hedgehog is required for progenitor cell maintenance in telencephalic stem cell niches. *Neuron* **39**, 937-950.

Merkle, F. T. and Alvarez-Buylla, A. (2006). Neural stem cells in mammalian development. *Curr. Opin. Cell Biol.* **18**, 704-709.

Mikawa, S., Wang, C. and Sato, K. (2006). Bone morphogenetic protein-4 expression in the adult rat brain. *J. Comp. Neurol.* **499**, 613-625.

Mirzadeh, Z., Merkle, F. T., Soriano-Navarro, M., Garcia-Verdugo, J. M. and Alvarez-Buylla, A. (2008). Neural stem cells confer unique pinwheel architecture to the ventricular surface in neurogenic regions of the adult brain. *Cell Stem Cell* **3**, 265-278.

Miyazono, K. and Miyazawa, K. (2002). Id: a target of BMP signaling. *Sci. STKE* **2002**, PE40.

Morshead, C. M., Reynolds, B. A., Craig, C. G., McBurney, M. W., Staines, W. A., Morassutti, D., Weiss, S. and van der Kooy, D. (1994). Neural stem cells in the adult mammalian forebrain: a relatively quiescent subpopulation of subependymal cells. *Neuron* **13**, 1071-1082.

Ninkovic, J. and Gotz, M. (2007). Signaling in adult neurogenesis: from stem cell niche to neuronal networks. *Curr. Opin. Neurobiol* **17**, 338-344.

Nolte, C., Matyash, M., Pivneva, T., Schipke, C. G., Ohlemeyer, C., Hanisch, U. K., Kirchhoff, F. and Kettenmann, H. (2001). GFAP promoter-controlled EGFP-expressing transgenic mice: a tool to visualize astrocytes and astrogliosis in living brain tissue. *Glia* **33**, 72-86.

Peretto, P., Dati, C., De Marchis, S., Kim, H. H., Ukhanova, M., Fasolo, A. and Margolis, F. L. (2004). Expression of the secreted factors noggin and bone morphogenetic proteins in the subependymal layer and olfactory bulb of the adult mouse brain. *Neuroscience* **128**, 685-696.

Reynolds, B. A. and Weiss, S. (1992). Generation of neurons and astrocytes from isolated cells of the adult mammalian central nervous system. *Science* **255**, 1707-1710.

Spoelgen, R., Hammes, A., Anzenberger, U., Zechner, D., Andersen, O. M., Jerchow, B. and Willnow, T. E. (2005). LRP2/megalin is required for patterning of the ventral telencephalon. *Development* **132**, 405-414.

Sur, M. and Rubenstein, J. L. (2005). Patterning and plasticity of the cerebral cortex. *Science* **310**, 805-810.

Willnow, T. E., Hilpert, J., Armstrong, S. A., Rohlmann, A., Hammer, R. E., Burns, D. K. and Herz, J. (1996). Defective forebrain development in mice lacking gp330/megalin. *Proc. Natl. Acad. Sci. USA* **93**, 8460-8464.

Yamaguchi, M., Saito, H., Suzuki, M. and Mori, K. (2000). Visualization of neurogenesis in the central nervous system using nestin promoter-GFP transgenic mice. *NeuroReport* **11**, 1991-1996.

Zarbalis, K., May, S. R., Shen, Y., Ekker, M., Rubenstein, J. L. and Peterson, A. S. (2004). A focused and efficient genetic screening strategy in the mouse: identification of mutations that disrupt cortical development. *PLoS Biol.* **2**, E219.

Zheng, G., Bachinsky, D. R., Stamenkovic, I., Strickland, D. K., Brown, D., Andres, G. and McCluskey, R. T. (1994). Organ distribution in rats of two members of the low-density lipoprotein receptor gene family, gp330 and LRP/alpa 2MR, and the receptor-associated protein (RAP). *J. Histochem. Cytochem.* **42**, 531-542.